nature physics

ARTICLES

PUBLISHED ONLINE: 23 MAY 2010 | DOI: 10.1038/NPHYS1668

Persistent currents and quantized vortices in a polariton superfluid

D. Sanvitto[1]*, F. M. Marchetti[2]*, M. H. Szymańska[3,4], G. Tosi[1], M. Baudisch[1], F. P. Laussy[5], D. N. Krizhanovskii[6], M. S. Skolnick[6], L. Marrucci[7], A. Lemaître[8], J. Bloch[8], C. Tejedor[2] and L. Viña[1]

After the discovery of zero viscosity in liquid helium, other fundamental properties of the superfluidity phenomenon have been revealed. One of them, irrotational flow, gives rise to quantized vortices and persistent currents. Those are the landmarks of superfluidity in its modern understanding. Recently, a new variety of dissipationless fluid behaviour has been found in microcavities under the optical parametric regime. Here we report the observation of metastable persistent polariton superflows sustaining a quantized angular momentum, *m*, after applying a 2-ps laser pulse carrying a vortex state. We observe a transfer of angular momentum to the steady-state condensate, which sustains vorticity for as long as it can be tracked. Furthermore, we study the stability of quantized vortices with $m = 2$. The experiments are analysed using a generalized two-component Gross–Pitaevskii equation. These results demonstrate the control of metastable persistent currents and show the peculiar superfluid character of non-equilibrium polariton condensates.

In the past few decades there has been a strenuous search for macroscopic coherence and phenomena related to Bose–Einstein condensation in the solid state. The first realization of a Bose–Einstein condensate (BEC) in semiconductor microcavities[1] has inaugurated a new era in the study of strongly coupled light–matter systems. The growing interest in this field can be attributed to the unique properties of exciton–polaritons in microcavities[2], the composite particles resulting from strong light–matter coupling. The properties of a polariton condensate[3] differ from those of other known condensates, such as ultracold atomic BECs and superfluid ^{4}He. In particular, polaritons have a short lifetime of the order of picoseconds, therefore needing continuous pumping to balance decay and reach a steady-state regime. Rather than a drawback, the intrinsic non-equilibrium nature enriches the features of polariton condensation, but at the same time poses fundamental questions about the robustness of the coherence phenomena to dissipation and non-equilibrium. Superfluid properties of non-equilibrium condensates in a dissipative environment still need to be understood[4]. In this work, to advance in this direction, we investigate the hallmark of superfluidity, namely, vortices and metastable persistent flows.

Polariton superfluid phases out of equilibrium

One route to inject polaritons into a microcavity is by non-resonant (incoherent) pumping. For incoherent pumping, polaritons have been shown to enter, within their short lifetime, a macroscopically coherent BEC phase[1,5,6]. However, the unusual form of the excitation spectrum—diffusive at small momenta—hinders the fulfilling of the Landau criterion and puts under debate the possibility of dissipationless superflow in incoherently pumped polariton systems[7–9]. As a result of the non-equilibrium nature of the polariton condensate in an inhomogeneous system, there are spontaneous supercurrents that may carry polaritons from gain- to loss-dominated regions. This can give rise to spontaneous formation of deterministic vortices, which do not necessarily imply superfluidity[4,10]. Another peculiarity of polariton systems is to be found in their polarization, giving rise to a nomenclature of half-vortices[11,12].

A different scenario characterizes coherent resonant injection of parametrically pumped polariton condensates, which have recently been shown to exhibit a new form of non-equilibrium superfluid behaviour[13,14]. In the optical parametric oscillator (OPO) regime[15], bosonic final-state stimulation causes polariton pairs to coherently scatter from the pump state to the signal and idler states, which, at threshold, have a state occupancy of order one. The properties of the quantum fluids generated by the OPO at idler and signal have recently been tested using a triggered optical parametric oscillator (TOPO) configuration[13]. Another weak pulsed probe laser beam has been used to create a travelling, long-living, coherent polariton signal, continuously fed by the OPO. The travelling signal has been shown to exhibit superfluid behaviour through frictionless flow. However, long-lived quantized vortices and metastable persistent flow, that is, another possible steady state of the condensate, still remained missing in the superfluid 'checklist'[4]. In this work, we fill in this gap and we also address the case of higher winding numbers, unravelling a rich dynamics of vortices in polariton condensates. For this purpose, we use a technique already applied in nonlinear and quantum optics, cold atoms and biophysics[16]: excitation by a light field carrying orbital angular momentum. Transfer of light orbital angular momentum has been demonstrated in parametric processes in nonlinear materials[17,18] and has been used to generate atomic vortex states in BECs (refs 19,20).

[1]Departamento de Física de Materiales, Universidad Autónoma de Madrid, Madrid 28049, Spain, [2]Departamento de Física Teórica de la Materia Condensada, Universidad Autónoma de Madrid, Madrid 28049, Spain, [3]Department of Physics, University of Warwick, Coventry CV4 7AL, UK, [4]London Centre for Nanotechnology, London WC1H 0AH, UK, [5]School of Physics and Astronomy, University of Southampton, Southampton SO17 1BJ, UK, [6]Department of Physics and Astronomy, University of Sheffield, Sheffield S3 7RH, UK, [7]Dipartimento di Scienze Fisiche, Università di Napoli Federico II and CNR-SPIN, Napoli 80126, Italy, [8]LPN/CNRS, Route de Nozay, 91460, Marcoussis, France. *e-mail: daniele.sanvitto@uam.es; francesca.marchetti@uam.es.

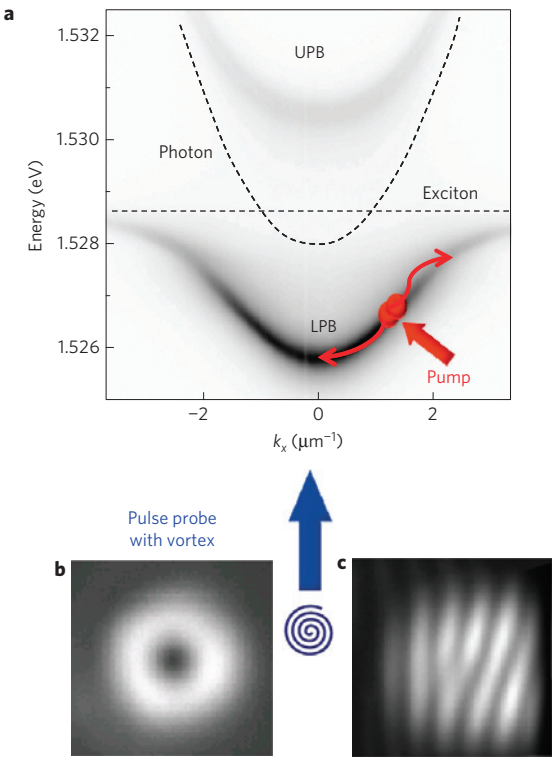

Figure 1 | Polariton dispersion, probe beam and its interference. a, Lower (LPB) and upper polariton branch (UPB) dispersions together with a schematic representation of the TOPO excitation. Resonantly pumping the lower polariton branch initiates, above threshold, stimulated scattering to a signal close to zero momentum and an idler at higher momentum. **b**, The $m=1$ Laguerre–Gauss beam resonant with the signal is used as a weak pulsed triggering probe to stir the superfluid. **c**, The corresponding interference image.

Generation of persistent currents

In our experiment, the vortex is excited by a pulsed probe resonant with the signal (Fig. 1) lasting only 2 ps. In other words, we stir the polariton superfluid for only a short time and observe its long-lived rotation with a quantum of angular momentum on a timescale almost 70 times longer than the duration of the pulse (Figs 2 and 3). Although there is a similarity with rotating trapped gases, the effect for driven, non-equilibrium systems shows a richer phenomenology as will be described in the rest of this article. Besides, a characteristic of vortices with a higher winding number m is the tendency to coherently split into many vortices of $m=1$ (ref. 21). To study the stability properties of vortices in polariton condensates, we have injected a vortex with $m=2$ and observed its evolution (Fig. 4). Surprisingly, we found three different behaviours depending on the initial condition. In cases for which the vortex is imprinted into the signal steady state, one topological charge is always expelled out of the condensate (Fig. 4g–i). On the other hand, when the vortex is not imprinted in the steady state but lasts only as long as the perturbation of the signal, we observe either a stable vortex of $m=2$ when the probe carrying the vortex is at small momentum, resulting in a static (or slowly moving) vortex and slow supercurrents, or a splitting into two vortices of $m=1$ when the vortex is injected with a probe at higher momentum. In the latter case, the vortex is moving faster than when it does not split, but still slower than the supercurrents of the condensate. Instability of doubly quantized vortices in a BEC has been observed in several systems[21], but there are only a few examples of their stability, such as in superconductors in the presence of pinning forces[22] or in a multicomponent order parameter superfluid such as ^{3}He–A (ref. 23). In ultracold atomic gases, stable free $m=2$ vortices have been theoretically predicted for some range of densities and interaction strengths[24]. However, they have been observed only in a toroidal pinning potential with an external optical plug[20], and demonstrated to split soon after the plug has been removed. The stability of $m=2$ static vortices in polariton systems provides a further experimental realization.

We use a semiconductor microcavity with a Rabi splitting $\Omega_R=4.4$ meV and the cavity photon energy slightly negatively detuned (between 1 and 3 meV) from the exciton energy; see the Methods section for details. A Ti:sapphire laser is tuned in resonance with the lower polariton branch, injecting polaritons close to the point of inflection and giving rise to a continuously pumped OPO (Fig. 1). Above a pump threshold, the signal generated close to zero momentum ($\mathbf{k}_s=0$) and the idler state at high momentum form an out-of-equilibrium coherent polariton superfluid. At a given time, we trigger a new scattering process on top of the OPO signal with a resonant pulsed probe. The size of the probe is smaller than that of the signal (by a factor $\approx$4) to allow free motion of the vortex within the condensate, thus avoiding a spurious confinement. The probe is a pulsed Laguerre–Gauss beam carrying a vortex of given angular momentum m, the phase of which winds around the vortex core with values from 0 to $2\pi m$. After a short time, $\sim$2 ps, the probe vanishes, leaving the polariton coherent state free to rotate, without the driving field. Although even a classical fluid acquires angular momentum in the presence of an external rotating drive, only a superfluid can exhibit infinitely-lived circulating flow in a dissipative environment once the external drive is turned off. To demonstrate persistence of the vortex angular momentum, we detect the phase pattern generated by making the polariton signal interfere with an expanded and flipped spatial region far from the vortex core (where the phase is approximately constant) in a Michelson interferometer. A fork-like dislocation with a difference of m arms corresponds to phase winding by $2\pi m$ around the vortex core (see Fig. 1b,c).

Vortex dynamics

Using a streak camera we can follow the evolution in time of the vortex generated by the pulsed probe. Time intervals of 4 ps are used to reconstruct two-dimensional images of the signal state after the perturbation has arrived. Every picture is the result of an average over many shots, all taken at the same time and same conditions. To separate the contribution of the signal from that of the pump, we filter, both in theory and experiments, the signal images in momentum space in a cone around $\mathbf{k}=0$ of approximately $\pm7°$. At time t_{pb}, the pulsed laser probe is shone on the sample. Its general effect is to enhance the polariton signal emission by a factor that ranges, depending on the experiment, between a few per cent to more than 100% with a delay of 10 ps after the pulse arrival time. At first a strong gain given by the presence of the probe creates an extra population on top of the OPO signal (called TOPO polaritons) before the OPO signal is re-established. We follow the evolution of the transient state and monitor how the probe affects the condensate in its steady state. We find that the original steady state can be recovered but also, more interestingly, that different stable solutions are possible.

The time evolution of an excited $m=1$ vortex and its interference pattern, which characterizes unequivocally the vortex state, are shown in Fig. 2, where the external probe has a power of 6.6 μW, which is less than the OPO signal emission before the probe arrives on the sample. In these images, we can observe two effects: immediately after the arrival of the probe, a vortex is generated in the TOPO polaritons and its vorticity is maintained although the population decays in a few tens of picoseconds. After the extra polaritons have disappeared, the vortex remains imprinted into the steady population of the condensate. Although the polariton

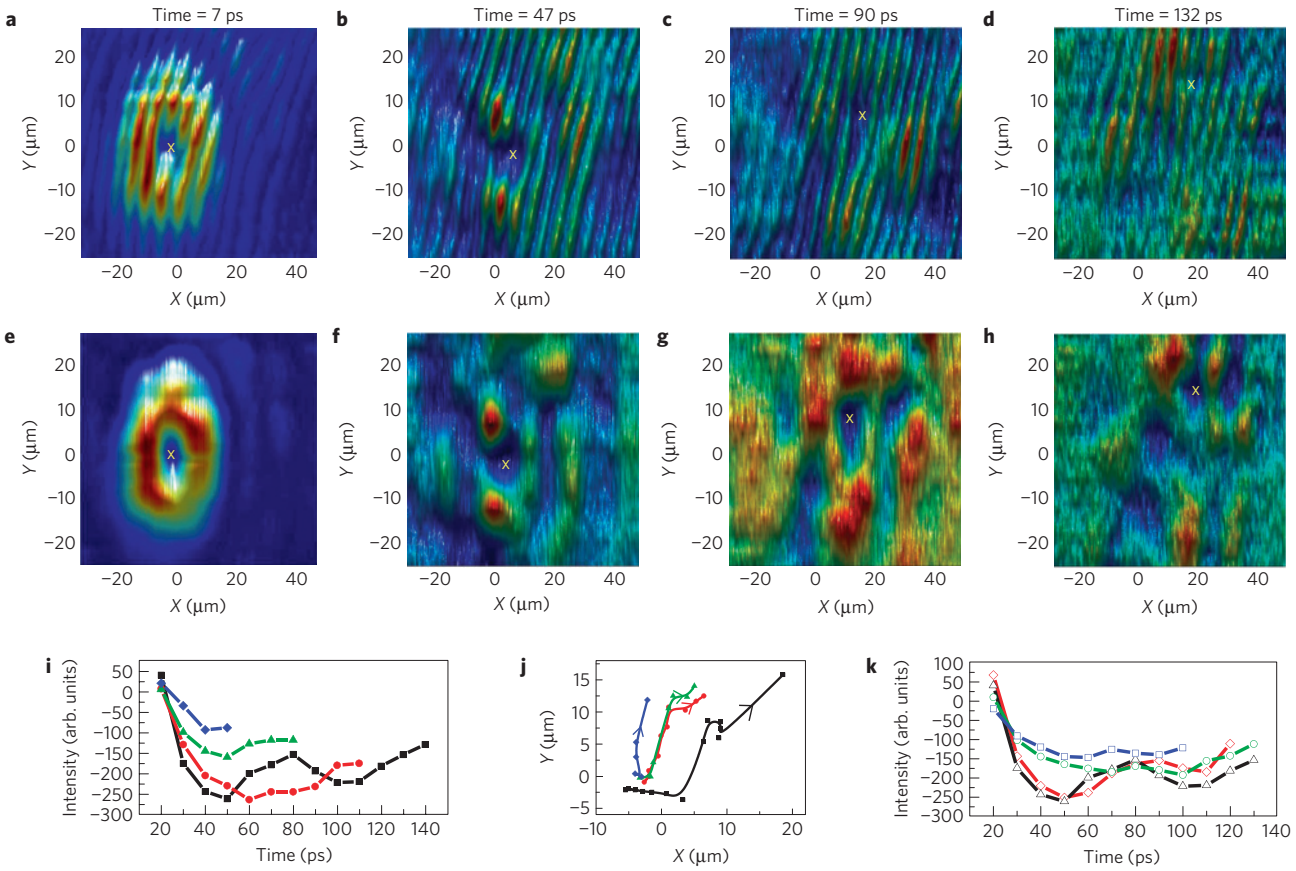

Figure 2 | Experimental dynamics of a single vortex. a–h, Time evolution of the polariton signal after a weak pulsed probe with a vortex of $m=1$ has been excited. The interference images (**a–d**) are obtained by overlapping the vortex with a small expanded region of the same image far from the vortex core, where the phase is constant. The time origin is taken when the extra population has reached 80% of its maximum value. To better reveal the effect of the imprinting of the vortex into the condensate steady state of the signal, the contribution of the unperturbed polariton signal (in the absence of the probe pulse) is subtracted from all data. Supplementary Videos S2(a–d) and S2(e–h) show the experimental dynamics of a single vortex. **i**,**j**, The depth of the vortex core (**i**) and its position (**j**) as a function of time for four different pump powers (65 mW, blue diamonds; 100 mW, green triangles; 200 mW, red circles; 300 mW, black squares)—all above the OPO threshold (50 mW). **k**, The effect of probe power—0.15 μW, blue squares; 0.33 μW, green circles; 6.65 μW, black triangles; 8 μW, red diamonds—on the duration and depth of the core of the vortex.

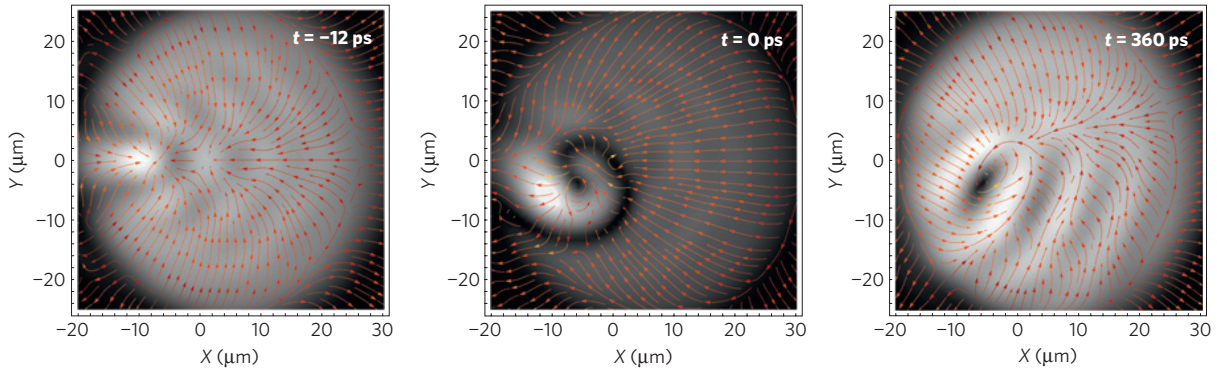

Figure 3 | Theoretical dynamics of a single vortex. Numerical simulations of the time evolution of the OPO signal before and after the arrival ($t=0$) of a pulsed probe carrying an $m=1$ vortex resonant with the signal momentum and energy, for pumping strength $f_p=1.24f_p^{(th)}$ above the OPO threshold. The images of the signal are obtained by momentum filtering in a cone of around ±7°. The pulse carrying the vortex generates a gain that fades out after about 10 ps leaving an $m=1$ vortex imprinted into the signal. The vortex experiences a transient time of around 30 ps before settling into a metastable solution. The supercurrents are plotted in the frame of the signal by subtracting the **k** of the signal. Supplementary Video S3 shows the calculated dynamics of a single vortex.

vorticity is always present and enduring in the TOPO polaritons, only under very high pump power and at specific points in the sample is the vorticity also passed to the steady state of the OPO signal. This not only demonstrates that polariton condensates show unperturbed rotation, but also that a vortex is another stable solution of the final steady state. This is a clear demonstration of superfluid behaviour in the non-equilibrium polariton OPO system. These effects are visible in the real-space images through

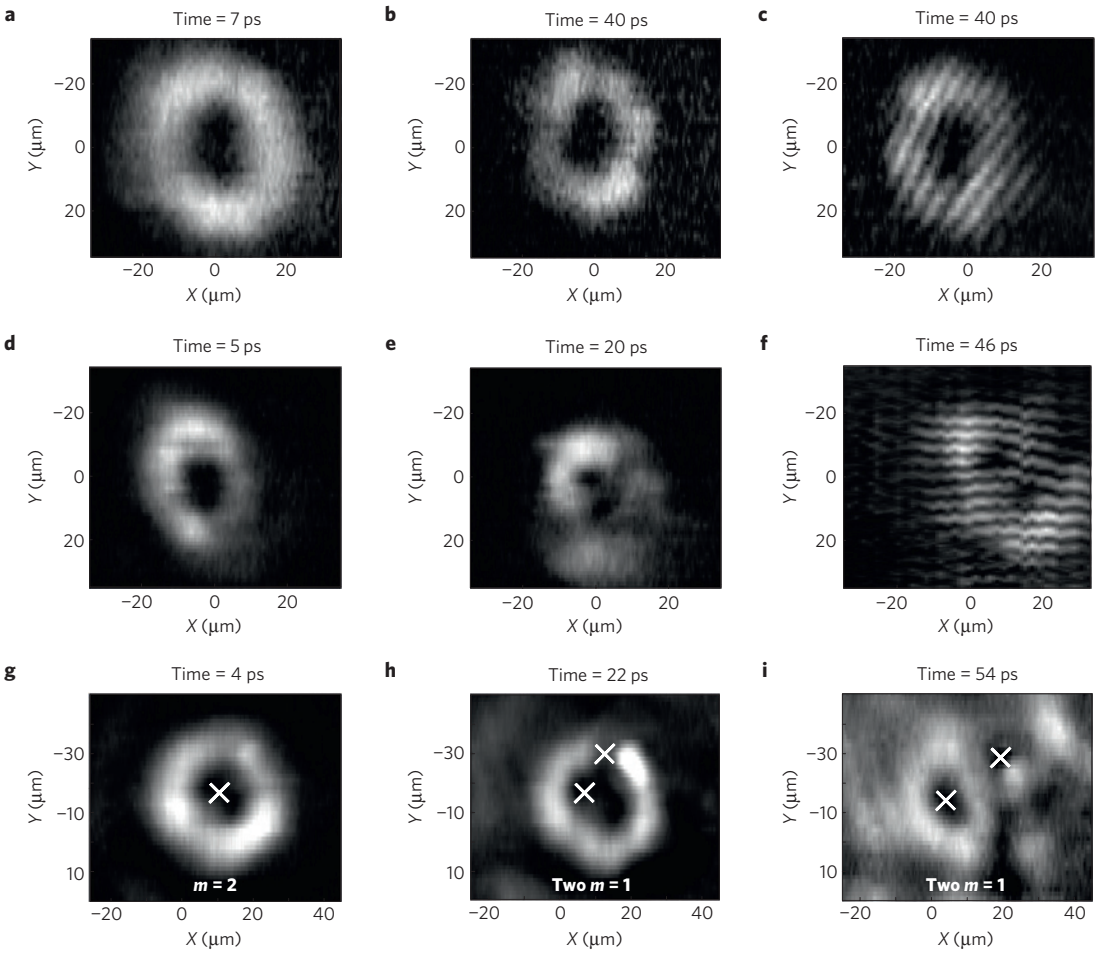

Figure 4 | Experimental dynamics of a doubly quantized vortex. a–c, Time evolution of an $m = 2$ vortex TOPO signal excited close to zero momentum, $\mathbf{k} = 0$, for which neither motion nor splitting of the vortex could be detected. **d–f**, However, for a signal at $\mathbf{k}_s$ pointing to the right, we can detect the $m = 2$ vortex both moving and splitting into two single quantized $m = 1$ vortices. **c** and **f** show the interference images corresponding to a late time. In both experiments the vortex is present only in the TOPO population. **g–i**, On the contrary, when the vortex is imprinted into the OPO state, then the situation is as shown in the images. Here the splitting appears immediately after the angular momentum is transferred to the steady state (≈20 ps) and only one of the two vortices of $m = 1$ survives, the other being expelled from the condensate in the first 40 ps. Supplementary Videos S4(c), S4(f), S4(g,i) and S4(g,i)-interferences show the experimental dynamics of a doubly quantized vortex.

the 'toroidal shape' of the polariton emission at early times, and the presence of a fork dislocation in the interference images at all times. The latter shows that the spatial phase relation remains constant and with full contrast all over a wide area, even for times much longer than the signal coherence time, as measured by detecting the decay of interference-fringe contrast when delaying the signal and the reference (Supplementary Fig. S6). This means that even when polaritons have lost any phase relation in time, their angular momentum is still conserved.

After the vortex is imprinted into the OPO signal, we can observe the vortex core slowly drifting to the right and then upwards changing in shape and moving with different velocities. The drift is due to the fact that the vortex core is naturally inclined to undergo a random walk and eventually either remains permanently trapped in the condensate or is expelled from the edges (see the following theory and ref. 25). However, owing to the presence of local defects[26], which tend to influence the motion of the vortex, the path followed by the vortex core recurs at each repetition of the experiment. For this reason we are able to track its movement that otherwise would be washed out by the experimental averaging.

Figure 2i–k shows the effect of pump and probe powers on the transfer of angular momentum to the condensate steady state. Note that to highlight this effect, all of the data shown in this article have been obtained by subtracting the steady state of the condensate unperturbed by the probe pulse. As a consequence, the depth of the vortex core comes out with negative values. An increase of the pump power helps the observation of this effect, possibly because of an enhancement of the OPO coherence for higher pumping intensities. Above four times the OPO threshold, we observe a saturation in the depth of the core (see intensity at 50 ps in Fig. 2i). However, given the different pathways followed by the vortex when changing pump intensity (Fig. 2j), a variation of the depth in time is also expected, depending on the kind of inhomogeneities met by the vortex along its trajectory. As for the probe, we find that a minimum power is required for the polaritons to acquire enough angular momentum to be able to transfer it to the steady state. This rigidity of the fluid to accommodate a vortex at low intensities has also been predicted for incoherently pumped polariton condensates[25]. However, once the transfer is achieved, the probe power does not change significantly the duration and depth of the vortex in the steady state. An alternative interpretation of the short vortex lifetime, for low excitation powers, could be attributed to dissipation when the average angular velocity is higher than some critical velocity—leading to the onset of macroscopic drag forces (such as recently discussed for non-resonant pumping in

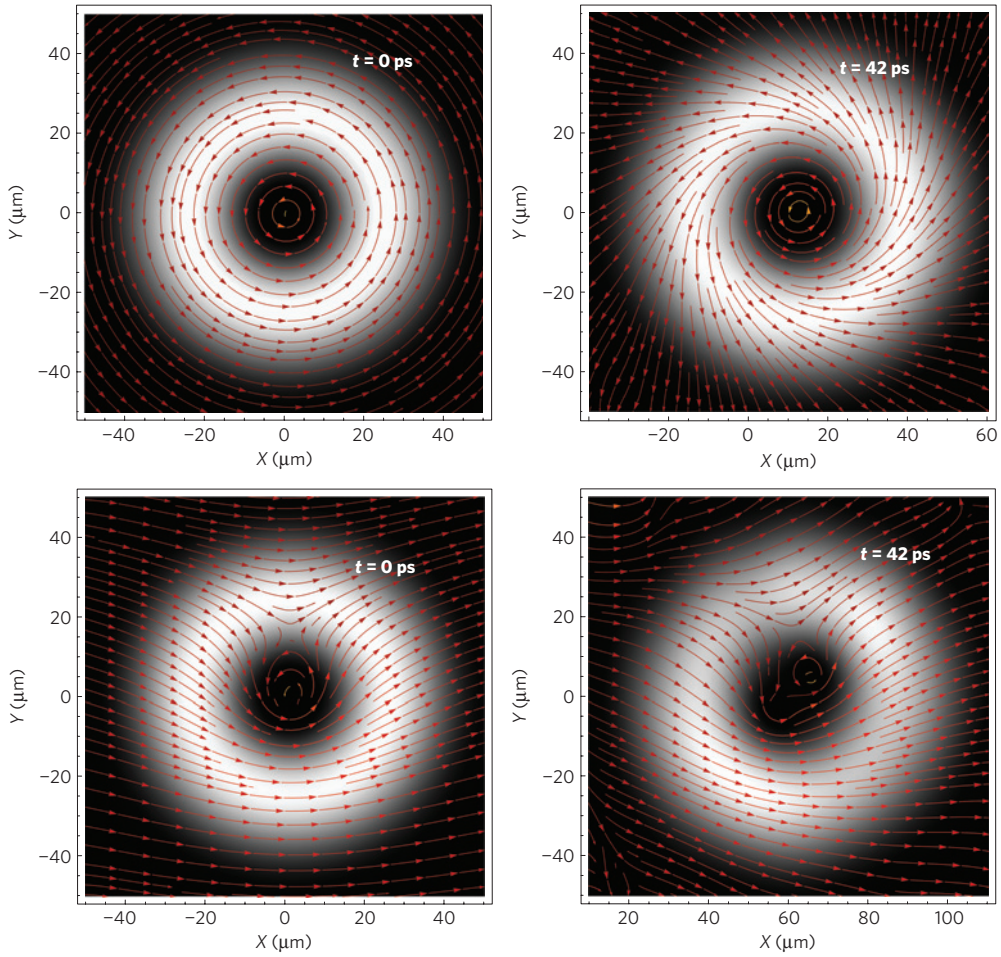

Figure 5 | Theoretical dynamics of a doubly quantized vortex. Calculated TOPO signal emission for an $m = 2$ triggering probe at $\mathbf{k}_{pb} = 0.1\,\mu m^{-1} < \mathbf{k}_{pb}{}^{cr}$ (first row) and at $\mathbf{k}_{pb} = 0.7\,\mu m^{-1} > \mathbf{k}_{pb}{}^{cr}$ (second row) at the arrival of the probe ($t = 0$) and 42 ps after. The supercurrents are plotted in the frame of the group velocity of the moving vortex. In the second row, the net current felt by the $m = 2$ vortex causes it to split (Supplementary Video S5).

ref. 9). Therefore, taking the difference between opposite momenta across the vortex core, we have obtained the average angular velocity to be $\sim 0.2\,\mu m\,ps^{-1}$. This value sets a lower bound for the critical velocity, which depends on polariton densities and, for small pumping powers, could be the cause of short lasting times for the polariton vorticity.

The sequence in Fig. 2 demonstrates that the vortex remains steady as a persisting metastable state for times much longer than the extra population created by the probe pulse and eventually gets imprinted in the steady state of the OPO signal. This is revealed by the strong contrast of the fork in the interference images for as long as the core remains within the condensate area. In the opposite scenario—dissipation of angular momentum as for classical fluids—the interference images would show low contrast in the vortex core region, indicating a mixture of the population that has undergone dissipation and the one still carrying the quantized angular momentum.

In our experiments we have measured an average size of the core radius between 4 and 5 μm. This is in good agreement with a theoretical estimate of the healing length $\xi \simeq \pi/\sqrt{2m_{LP}\delta E}$, where m_{LP} is the lower polariton mass and δE is the lower polariton blueshift, determined by the polariton–polariton interaction strength.

Numerical simulations

We have numerically simulated the experiments by making use of mean-field two-component Gross–Pitaevskii equations for the coupled cavity and exciton fields with external pumping and decay; see the Methods section for details. We have chosen parameters close to the experimental ones, finding first the conditions for the OPO. In the simulation of Fig. 3, we consider a pump with strength $f_p = 1.24 f_p{}^{(th)}$ above the OPO threshold, and once the steady state is reached (left panel), we turn on the probe carrying a vortex $m = 1$, resonant with the signal for only 2 ps. We observe a gain of the signal (central panel) for around 10 ps, which is followed by a transient time during which the imprinted vortex drifts around inside the signal. For the simulation shown in Fig. 3, the transient lasts for about 30 ps, after which the vortex settles into a metastable solution lasting around 400 ps. In addition, we also find stable steady-state (that is, infinitely lived) vortex solutions, analogous to the ones reported in ref. 27. Such a solution does not always exist and it strongly depends on the pumping conditions: in other cases, during the transient period, the excited vortex either spirals out of the signal or recombines with an antivortex forming at the edge of the signal. There are also cases where, instead, the imprinted vortex settles into a metastable state, which can last several hundred picoseconds as shown in Fig. 3, and then starts drifting again. We have also analysed the dependence of the vortex solutions on the probe intensity and found that for steady-state vortex solutions there is no dependence on the probe intensity, which can affect only the duration of the transient period. However, for metastable solutions, we found a threshold in the probe power, below which the vortex does not get imprinted into the signal anymore. Thus, the results of the theoretical simulations are in excellent qualitative agreement with the experimental observations.

Doubly quantized vortices

A second experiment is aimed at investigating the stability of doubly quantized vortices in different regimes. We carry out both experiments and numerical simulations in conditions similar to the ones previously described, but now considering a pulsed probe carrying a doubly quantized vortex $m=2$. We demonstrate three distinctive behaviours (Fig. 4) by repeating the experiments under different conditions. For cases in which the vortex lasts as long as the TOPO population is present, we observe that when the vortex is excited on a static signal centred at $\mathbf{k}=0$, it does not split within its lifetime (Fig. 4a–c). However, exciting the signal with a finite momentum, thus making it move inside the pump spot, we observe the doubly quantized vortex splitting into two singly quantized vortices, as shown in Fig. 4d–f.

Our theoretical analysis gives the same result: a TOPO vortex (below the OPO threshold) is stable when it is either at rest or moves below a critical velocity, and splits otherwise (Fig. 5). To explain this result, we have analysed the supercurrents characterizing the signal. We found that, below threshold, these supercurrents are a superposition of the vortex currents with a net current corresponding exactly to the momentum $\mathbf{k}_{\rm pb}$ at which the probe has been injected. In addition, we have evaluated the group velocity $\mathbf{v}_{\rm g}$ at which the triggered signal (carrying the vortex) moves in real space. We found that $\mathbf{v}_{\rm g}$ increases linearly with $\mathbf{k}_{\rm pb}$ up to a critical value, $\mathbf{k}_{\rm pb}{}^{\rm cr}$, and sublinearly above. Therefore, we expect that in the frame of the moving vortex, there is no net current in the linear regime, whereas, in the sublinear regime, the vortex feels a net current that causes it to split (Fig. 5). Indeed, we observe that the $m=2$ vortex splits exactly when it is injected at or above $\mathbf{k}_{\rm pb}{}^{\rm cr}$. Note that a TOPO signal is a decaying state; therefore, the $m=2$ vortex can be stable only within its lifetime.

In the case when, instead, the vortex is also imprinted into the OPO steady state, we observe that the $m=2$ vortex splits, one $m=1$ vortex is quickly expelled outside the signal, whereas the other vortex stabilizes and persists, as is also the case in the experiment (see Fig. 4g,i). Numerical simulations show that above the OPO threshold the structure of the currents in the signal is complex and thus a stationary vortex will always feel a net current. This is the reason why above the OPO threshold we always observe splitting of the $m=2$ vortex.

Methods

Experiments. The sample studied is a $\lambda/2$ AlAs microcavity with a 20 nm GaAs quantum well placed at the antinode of the cavity electromagnetic field. The cavity is formed by two highly reflective Bragg mirrors of 25 pairs at the bottom and 15.5 on the top of the structure. The pump is obtained with a continuous-wave (c.w.) Ti:sapphire laser, resonantly exciting the lower polariton branch close to the inflection point at 9°. The spot size is of ≈100 μm.

The experiments are carried out at a cryogenic temperature of 10 K and using a very high numerical-aperture lens (0.6) so that the sample can be accessed by angles as large as 25° and the photoluminescence can be simultaneously collected from the signal state in the near as well as the far field. The photoluminescence was collected through a 0.5 m spectrometer into a streak camera, working in synchroscan mode, with 4 ps time resolution, allowing for energy—as well as time-resolved—images. To reach a high time resolution, all of the images were obtained by filtering the signal in the far field without spectrally resolving the emission of the OPO states. Differently from our TOPO experiment[28], here we excite and trigger with the probe at the signal state in a pumping regime above threshold.

The vortex probe state is prepared by scattering a Ti:sapphire pulsed laser Gaussian beam in a hologram with a single or double fork-like dislocation. This gives rise to a first-order Laguerre–Gauss beam with a winding number of either $m=1$ or $m=2$, respectively. The probe beam is focused at the centre of the c.w. pump in resonance with the signal emission energy and at around $\mathbf{k}=0$ for most of the cases, except when a finite velocity is given to the vortex state. In this latter case the probe is arriving on the sample with a finite angle, between one and two degrees, so that the vortex can have a finite velocity showing splitting of the $m=2$ state. The probe is focused in a region of ≈25 μm having a power set to be below the intensity of the signal. Moreover, considering the wide energy spread given by its fast duration (2 ps), the amount of power getting into the cavity is estimated to be between 1/10 and 1/5 of the signal emission. Every picture is the result of an average over many shots, as single-shot measurements would give a too low signal-to-noise ratio.

A realization of optically transferring orbital angular momentum to atomic BECs, using Laguerre–Gauss beams, as in our experiments, was carried out using a two-photon stimulated Raman process[19]. $m=2$ vortices were generated in a BEC of sodium atoms but its stability was not analysed.

Theory. The dynamics of amplitudes and phases of the TOPO is analysed using a two-component Gross–Pitaevskii equation with external pumping and decay for the coupled cavity and exciton fields $\psi_{\rm C,X}(\mathbf{r},t)$ ($\hbar=1$):

$$i\partial_t\begin{pmatrix}\psi_{\rm X}\\ \psi_{\rm C}\end{pmatrix}=\begin{pmatrix}\omega_{\rm X}-i\kappa_{\rm X}+g_{\rm X}|\psi_{\rm X}|^2 & \Omega_{\rm R}/2\\ \Omega_{\rm R}/2 & \omega_{\rm C}-i\kappa_{\rm C}\end{pmatrix}\begin{pmatrix}\psi_{\rm X}\\ \psi_{\rm C}\end{pmatrix}+\begin{pmatrix}0\\ F_{\rm p}+F_{\rm pb}\end{pmatrix} \quad (1)$$

As the exciton mass is four orders of magnitude larger than the photon mass, we neglect the excitonic dispersion and assume a quadratic dispersion for the cavity photon, $\omega_{\rm C}=\omega_{\rm C}(0)-\nabla^2/2m_{\rm C}$. The fields decay with rates $\kappa_{\rm C,X}$. $\Omega_{\rm R}$ is the photon–exciton coupling. The cavity field is driven by an external c.w. pump field,

$$F_{\rm p}(\mathbf{r},t)=f_{\rm p}\,{\rm e}^{-\frac{|\mathbf{r}-\mathbf{r}_{\rm p}|^2}{2\sigma_{\rm p}^2}}\,{\rm e}^{i(\mathbf{k}_{\rm p}\cdot\mathbf{r}-\omega_{\rm p}t)}$$

and the probe is a Laguerre–Gaussian pulsed beam,

$$F_{\rm pb}(\mathbf{r},t)\simeq f_{\rm pb}|\mathbf{r}-\mathbf{r}_{\rm pb}|^m\,{\rm e}^{-\frac{|\mathbf{r}-\mathbf{r}_{\rm pb}|^2}{2\sigma_{\rm pb}^2}}\,{\rm e}^{im\varphi(\mathbf{r})}\,{\rm e}^{-\frac{(t-t_{\rm pb})^2}{2\sigma_t^2}}\,{\rm e}^{i(\mathbf{k}_{\rm pb}\cdot\mathbf{r}-\omega_{\rm pb}t)} \quad (2)$$

producing a vortex at $\mathbf{r}_{\rm pb}$ with winding number m. The exciton repulsive interaction strength $g_{\rm X}$ can be set to one by rescaling fields and pump strengths. We solve equation (1) numerically by using the fifth-order adaptive-step Runge–Kutta algorithm on a two-dimensional grid.

We take $m_{\rm C}=2.3\times10^{-5}m_0$ and a Rabi splitting $\Omega_{\rm R}=4.4$ meV determined experimentally. In the regime of our experiments, we can neglect the saturation of the dipole coupling[29]. We choose the pumping angle $\mathbf{k}_{\rm p}$, the energy of the pump $\omega_{\rm p}$ and the pump profile as the experimental ones.

The calculated images of the signal in Figs 3 and 5 are obtained by filtering in momentum space around the signal momentum, $\mathbf{k}_{\rm s}$. We set to zero all of the emission in momentum space except the one coming from the signal and fast Fourier transform back to real space. In this way the strong emission coming at the pump angles is masked out.

Received 31 July 2009; accepted 12 April 2010; published online 23 May 2010

References

1. Kasprzak, J. *et al.* Bose–Einstein condensation of exciton polaritons. *Nature* **443,** 409–414 (2006).
2. Weisbuch, C., Nishioka, M., Ishikawa, A. & Arakawa, Y. Observation of the coupled exciton–photon mode splitting in a semiconductor quantum microcavity. *Phys. Rev. Lett.* **69,** 3314–3317 (1992).
3. Keeling, J., Marchetti, F. M., Szymańska, M. H. & Littlewood, P. B. Collective coherence in planar semiconductor microcavities. *Semicond. Sci. Technol.* **22,** R1–R26 (2006).
4. Keeling, J. & Berloff, N. G. Going with the flow. *Nature* **457,** 273–274 (2009).
5. Balili, R., Hartwell, V., Snoke, D., Pfeiffer, L. & West, K. Bose–Einstein condensation of microcavity polaritons in a trap. *Science* **316,** 1007–1010 (2007).
6. Lai, C. W. *et al.* Coherent zero-state and π-state in an exciton–polariton condensate array. *Nature* **450,** 529–532 (2007).
7. Szymańska, M. H., Keeling, J. & Littlewood, P. B. Nonequilibrium quantum condensation in an incoherently pumped dissipative system. *Phys. Rev. Lett.* **96,** 230602 (2006).
8. Wouters, M. & Carusotto, I. Excitations in a nonequilibrium Bose–Einstein condensate of exciton polaritons. *Phys. Rev. Lett.* **99,** 140402 (2007).
9. Wouters, M. & Carusotto, I. Are non-equilibrium Bose–Einstein condensates superfluid? Preprint at http://www.arxiv.org/abs/1001.0660 (2010).
10. Lagoudakis, K. G. *et al.* Quantised vortices in an exciton–polariton fluid. *Nature Phys.* **4,** 706–710 (2008).
11. Rubo, Y. G. Half vortices in exciton polariton condensates. *Phys. Rev. Lett.* **99,** 106401 (2007).
12. Lagoudakis, K. G. *et al.* Observation of half-quantum vortices in an exciton–polariton condensate. *Science* **326,** 974–976 (2009).
13. Amo, A. *et al.* Collective fluid dynamics of a polariton condensate in a semiconductor microcavity. *Nature* **457,** 291–295 (2009).
14. Amo, A. *et al.* Superfluidity of polaritons in semiconductor microcavities. *Nature Phys.* **5,** 805–810 (2009).
15. Stevenson, R. M. *et al.* Continuous wave observation of massive polariton redistribution by stimulated scattering in semiconductor microcavities. *Phys. Rev. Lett.* **85,** 3680–3683 (2000).
16. Molina-Terriza, G., Torres, J. P. & Torner, L. Twisted photons. *Nature Phys.* **3,** 305–310 (2007).

17. Dholakia, K., Simpson, N. B., Padgett, M. J. & Allen, L. Second harmonic generation and the orbital angular momentum of light. *Phys. Rev. A* **54,** R3742–R3745 (1996).
18. Martinelli, M., Huguenin, J. A. O., Nussenzveig, P. & Khuory, A. Z. Orbital angular momentum exchange in an optical parametric oscillator. *Phys. Rev. B* **70,** 013812 (2004).
19. Andersen, M. F. *et al.* Quantized rotation of atoms from photons with orbital angular momentum. *Phys. Rev. Lett.* **97,** 170406 (2006).
20. Ryu, C. *et al.* Observation of persistent flow of a Bose–Einstein condensate in a toroidal trap. *Phys. Rev. Lett.* **99,** 260401 (2007).
21. Shin, Y. *et al.* Dynamical instability of a doubly quantized vortex in a Bose–Einstein condensate. *Phys. Rev. Lett.* **93,** 160406 (2004).
22. Baert, M., Metlushko, V. V., Jonckheere, R., Moshchalkov, V. V. & Bruynseraede, Y. Composite flux-line lattices stabilized in superconducting films by a regular array of artificial defects. *Phys. Rev. Lett.* **74,** 3269–3272 (1995).
23. Blaauwgeers, R. *et al.* Double-quantum vortex in superfluid 3He–A. *Nature* **404,** 471–473 (2000).
24. Möttönen, M., Mizushima, T., Isoshima, T., Salomaa, M. M. & Machida, K. Splitting of a doubly quantized vortex through intertwining in Bose–Einstein condensates. *Phys. Rev. A* **68,** 023611 (2003).
25. Wouters, M. & Savona, V. Creation and detection of vortices in polariton condensates. *Phys. Rev. B* **81,** 054508 (2010).
26. Sanvitto, D. *et al.* Spatial structure and stability of the macroscopically occupied polariton state in the microcavity optical parametric oscillator. *Phys. Rev. B* **73,** 241308 (2006).
27. Whittaker, D. Vortices in the microcavity optical parametric oscillator. *Superlattices Microstruct.* **41,** 297–300 (2007).
28. Ballarini, D. *et al.* Observation of long-lived polariton states in semiconductor microcavities across the parametric threshold. *Phys. Rev. Lett.* **102,** 056402 (2009).
29. Ciuti, C., Schwendimann, P. & Quattropani, A. Theory of polariton parametric interactions in semiconductor microcavities. *Semicond. Sci. Technol.* **18,** S279–S293 (2003).

Acknowledgements

We are grateful to D. Whittaker, J. J. García-Ripoll, P. B. Littlewood and J. Keeling for stimulating discussions. This work was partially supported by the Spanish MEC (MAT2008-01555 and QOIT-CSD2006-00019), the CAM (S2009/ESP-1503), FP7 ITNs 'Clermont4' (235114) and 'Spin-Optronics' (237252). D.S. and F.M.M. acknowledge financial support from the Ramón y Cajal programme. G.T. is grateful for the FPI scholarship from the Ministerio de Ciencia e Innovación. We thank the TCM group (Cavendish Laboratory, Cambridge, UK) for the use of computer resources.

Author contributions

D.S., G.T. and M.B. carried out the experiments. F.M.M. and M.H.S. carried out the theoretical analysis. L.M. provided the holograms for getting vortex excitation and A.L. and J.B. fabricated the samples. All of the authors analysed the results, discussed the underlying physics and contributed to the manuscript.

Additional information

The authors declare no competing financial interests. Supplementary information accompanies this paper on www.nature.com/naturephysics. Reprints and permissions information is available online at http://npg.nature.com/reprintsandpermissions. Correspondence and requests for materials should be addressed to D.S. (for experimental details) and F.M.M. (for theoretical matters).